Progress In Electromagnetics Research B, Vol. 63, 275–288, 2015

Electrodynamic Characteristics of Horizontal Impedance Vibrator Located over a Finite-Dimensional Perfectly Conducting Screen

Nadezhda P. Yeliseyeva, Sergey L. Berdnik,
Victor A. Katrich, and Mikhail V. Nesterenko*

Abstract—A problem of electromagnetic waves radiation by an impedance vibrator located over finite-dimensional perfectly conducting screen is solved. The vibrator may have surface impedance distributed over its length. The solution is derived using asymptotic expressions for the current in a horizontal impedance vibrator placed over an infinite plane, obtained by averaging method. The problem was solved provided that the diffracted fields from the edges of the screen have little effect on the vibrator current amplitude, i.e., if the screen dimensions are comparable to or larger than the wavelength. Full radiation fields in all observation space in the far zone were found by the uniform geometrical theory of diffraction. The vibrator dimensions, value and type of surface impedance, removing from the screen and screen sizes were used as parameters. The multivariable electrodynamic characteristics of the resonant impedance vibrators placed above an infinite plane and square screen were studied. Characteristics dependences upon the vibrator dimensions, value and type of the surface impedance, removing from the screen, and screen dimensions were obtained.

1. INTRODUCTION

For solving the problem of diffraction of electromagnetic waves on material bodies, with characteristic dimensions much larger than the wavelength, the concept of the diffracted rays was successfully used, and geometrical theory of diffraction (GTD) was developed by Keller [1–3]. An analysis of the short-wavelength asymptotics of the known rigorous solutions of the problem of diffraction of electromagnetic waves on a wedge, cylinder, sphere has shown that an infringement of the laws of geometrical optics (GO) occurs only in the narrow transition zones where there are excited diffracted fields. Propagation of these fields away from the excitation region is determined by the laws of GO. Both GO and GTD laws are local, i.e., fields on the adjacent rays do not interact. Therefore, Keller had found diffraction coefficients using the exact solution of the model problem, which has the same local features of the body geometry and the geometry of the incident wave front. The basic idea of this theory is that the solution is determined everywhere, except the narrow transition zones in vicinity of the light-shadow boundary of the GO waves as a sum of the fields satisfying the first approximation GO. However, the GO field should be corrected by the diffraction terms corresponding to the short-wavelength asymptotic expansion for the exact solution of the model diffraction problem. Field at any point in space (in the Fresnel and Fraunhofer zones) outside the transition zone can be calculated using the formulas for the edge wave fields and diffraction coefficients. The field in the transition zones (half-shadow field) is expressed by the special functions obtained from the analysis of model problem.

The transition zones for the electromagnetic waves diffraction on bodies, with characteristic dimensions comparable with the wavelength, are expanding. Therefore, for numerical calculation, one

Received 30 April 2015, Accepted 8 October 2015, Scheduled 19 October 2015
* Corresponding author: Mikhail V. Nesterenko (mikhail.v.nesterenko@univer.kharkov.ua).
The authors are with the Department of Radiophysics, V. N. Karazin Kharkov National University, 4, Svobody Sq., Kharkov 61022, Ukraine.

can use uniform diffraction coefficients suitable for both the far and near light-shadow boundaries of GO waves. Thus, the GTD development can be divided into two stages: the ray representation of the diffracted fields and uniform geometrical theory of diffraction (UGTD). Uniform diffraction coefficients at the edge of a perfectly conducting half-plane for the cases when the source is an elementary electric or magnetic dipole with axes parallel to the edge of the half-plane were defined in [4, 5]. These coefficients are continuous for any angular coordinates defining the position of the source and observation points. The matrix form of the uniform diffraction coefficient for the diffraction problem of the arbitrarily oriented electric Hertz dipole field at the edge of the half-plane was obtained in [6, 7].

The UGTD developed in [6] for three-dimensional diffraction problems of an arbitrarily oriented perfectly conducting half-wave vibrator field on the perfectly conducting infinitely thin finite size rectangular screen, and on the corner reflectors of various configurations, has been used to calculate the amplitude and polarization patterns of radiating systems. Experimental studies in the centimeter wavelength [6, 8] have confirmed the high degree of reliability of the radiation patterns calculated by UGTD method for half-wave vibrator over the rectangular screen, with sides equal to the wavelength.

Electrodynamics characteristics of vibrators with constant and variable along their length surface impedance distribution were studied in [9, 10]. The vibrator can be located in an unbounded material medium and over an infinite perfectly conducting plane. It has been shown that the vibrator with fixed geometrical dimensions can be resonant tuned using the distributed inductive or capacitive surface impedance. Thus, the length of the vibrator can be less or greater than half of the operating wavelength. In the present paper, on the base of asymptotic solution of the integral equation for the current in the horizontal impedance vibrator located above the infinite plane, we will find the field of such a vibrator placed above a rectangular screen in all observation space in the far zone using UGTD. This structure is considered the first time and creates new opportunities for formation electromagnetic fields with the specified characteristics. The multivariable electrodynamic characteristics of the resonant impedance vibrators above an infinite plane and square screen were studied. Dependences of the characteristics upon the vibrator dimensions, value and type of the surface impedance, removing from the screen, and screen dimensions were obtained.

2. PROBLEM FORMULATION

Let us consider a radiating system consisting of a thin impedance vibrator placed over a perfectly conducting infinitely thin rectangular screen, with sides L and W. The vibrator radius is r, and its length is $2l$. The vibrator is located at a distance h above the middle of the screen. Let us introduce a Cartesian coordinate system XYZ, with origin O in the middle of the screen and a spherical coordinate system $\tilde{R}, \theta, \varphi$, wherein the angles φ and θ are measured from the axes X, and Z, respectively (Fig. 1). For an arbitrary orientation of the vibrator relative to the screen, the angle between the vibrator axis and its projection on the plane XY is ν, and the angle between the vibrator axis projection onto the plane XY andaxis X is ζ. In Fig. 1, the vibrators **1**, **2** and **3** are directed along axes Z, Y and X, respectively.

In accordance with the method UGTD ($k \to \infty$, $k = 2\pi/\lambda$ is the wave number and λ the wavelength in free space), the field $E(\theta, \varphi)$ of radiating system in the far zone using the primary diffraction approximation is the sum of incident ($p = 1$) and reflected ($p = 2$) GO fields of spherical waves E_p, and the fields $E_{D_{pn}}$ of once diffracted waves excited by the incident and reflected waves at each n-th edge of the screen ($n = 1 \div 4$), and can be presented as

$$E(\theta, \varphi) = \sum_{p=1}^{2} E_p \chi_p + \sum_{n=1}^{4} \sum_{p=1}^{2} E_{D_{pn}} \chi_{pn}. \tag{1}$$

Since the screen dimensions are finite, each field has its own regions of light and shadow, whose boundary equations in all observation space in the far zone are defined in [6]. In expression (1), shading coefficients χ_p, χ_{pn} are equal to one and zero in the light and shadow regions of the incident, reflected and eight diffracted waves, respectively.

In [11–13], the radiation patterns (RP) of the incident and reflected waves were calculated using expressions for the far field of a thin perfectly conducting vibrator with sinusoidal current distribution

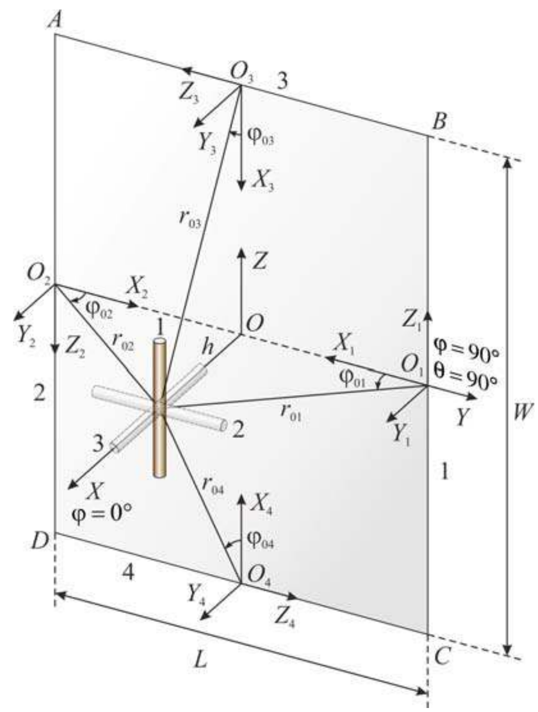

Figure 1. Geometry of the problem and notations.

$J(z) = J_0 \sin k(l - |z|)$, where J_0 is the current amplitude. Now, we have used a thin vibrator as a radiator distributed along its length surface impedance. Before finding the far GO field E_p and diffracted fields $E_{D_{pn}}$ for the impedance vibrator, we will focus on determining the current distribution on the impedance vibrator, located in free space and above an infinite plane.

3. SOLVING THE EQUATION FOR CURRENT ON A THIN IMPEDANCE VIBRATOR PLACED IN AN ARBITRARY ELECTRODYNAMIC VOLUME

Let a cylindrical conductor (vibrator) placed in an arbitrary electrodynamic volume bounded by a smooth surface. The radius of the vibrator is r, and its length is $2l$. The vibrator is excited by the field of extraneous sources $\vec{E}_0(\vec{r})$, and $\vec{r}$ is the radius-vector of the observation point. The time dependence is $e^{i\omega t}$, and ω is the angular frequency. Material parameters of media filling the volume, dielectric permittivity and magnetic permeability, are ε_1 and μ_1, respectively.

The vibrator is characterized by distributed surface impedance, which may be non-uniform along its length. Since the vibrator is thin, following inequalities

$$\frac{r}{2l} \ll 1, \quad \left|\frac{r}{\lambda_1}\right| \ll 1 \tag{2}$$

hold. Here λ_1 is the wavelength in the medium. The starting point for the analysis is a quasi-one-dimensional integral equation for the current in a vibrator [9, 10]

$$\left(\frac{d^2}{ds^2} + k_1^2\right) \int_{-l}^{l} J(s') G_s^V(s, s') ds' = -i\omega\varepsilon_1 E_{0s}(s) + i\omega\varepsilon_1 z_i(s) J(s), \tag{3}$$

Here s is the local coordinate associated with the axis of the vibrator, $k_1 = k\sqrt{\varepsilon_1 \mu_1}$ the wave number in the medium, $G_s^V(s, s')$ the s-component of the tensor Green's function of the electric type for the volume V, $E_{0s}(s)$ the projection of extraneous sources on the vibrator axis, and $z_i(s)$ an internal linear impedance of the vibrator ([Ohm/m])

$$\hat{G}^V(\vec{r},\vec{r}') = \hat{I}\frac{e^{-ik_1|\vec{r}-\vec{r}'|}}{|\vec{r}-\vec{r}'|} + \hat{G}_0^V(\vec{r},\vec{r}'), \tag{4}$$

where $\hat{I}\frac{e^{-ik_1|\vec{r}-\vec{r}'|}}{|\vec{r}-\vec{r}'|}$ is the Green's function of an unbounded space, $\hat{I}$ the unit tensor, $\vec{r}'$ the radius-vector of the source point, and $\hat{G}_0^V(\vec{r},\vec{r}')$ the regular function satisfying the homogeneous equation [14]

$$\Delta\hat{G}_0^V\left(\vec{r},\vec{r}'\right) + k_1^2\hat{G}_0^V\left(\vec{r},\vec{r}'\right) = 0 \tag{5}$$

and guarantees, together with $\hat{I}G(\vec{r},\vec{r}')$, the fulfillment of boundary conditions on the surface volume for the field of a point source located at $\vec{r}'$. If S is an infinite perfectly conducting plane, the Green's function (4) can be constructed in two ways: by the mirror image method or by the eigenfunctions method [15]. These methods from the point of view concerning the physical interpretation are equivalent. The advantage of the mirror image method is its obviousness, especially when V is half-space over a perfectly conducting plane. However, this method is not always possible to be applied to other geometries of volume V, and practical calculations, which in many cases, leads to a relatively complex analytical expressions. The eigenfunctions method is more general and applicable to various forms of volume V, for example, for cylindrical waveguides and resonators [10], spherical resonators, unlimited space outside the bodies of different configurations [16], etc. Using the eigenfunctions method we can write

$$G_s^V(s,s') = \frac{e^{-ik_1\sqrt{(s-s')^2+r^2}}}{\sqrt{(s-s')^2+r^2}} + G_{0s}^{Hs}(s,s') + G_{0s}^D(s,s'), \tag{6}$$

where $\frac{e^{-ik_1\sqrt{(s-s')^2+r^2}}}{\sqrt{(s-s')^2+r^2}} = \frac{e^{-ik_1R(s,s')}}{R(s,s')} = G_s^{Fs}(s,s')$ kernel of the integral equation for the vibrator in an unbounded space corresponding thin wire approximation [17], the function $G_{0s}^{Hs}(s,s')$ corresponds to the presence of an infinite perfectly conducting plane located at a distance h from the vibrator axis, and the function $G_{0s}^D(s,s')$ is defined by the waves diffraction on the edges of the screen.

3.1. Impedance Vibrator in the Free Space and over the Infinite Ideally Conducting Plane

The solution of the equation for the current in the free space ($\varepsilon_1 = \mu_1 = 1$) for $z_i = \text{const}$ was obtained in [9, 10] by asymptotic method of averaging within the accuracy of order α^2, ($\alpha = \frac{1}{2\ln[r/(2l)]}$ is a natural small parameter of the problem, $|\alpha| \ll 1$). The symmetric (index "s") and antisymmetric (index "a") current components, for an arbitrary vibrator excitation, have the form

$$\begin{aligned} J(s) \;=\; J^s(s) + J^a(s) = \alpha\frac{i\omega}{k}\Bigg\{ & \int_{-l}^{s} E_{0s}(s')\sin\tilde{k}(s-s')\,ds' \\ & -\frac{\sin\tilde{k}(l+s)}{\sin 2\tilde{k}l + \alpha P^s(kr,2\tilde{k}l)}\int_{-l}^{l} E_{0s}^s(s')\sin\tilde{k}(l-s')\,ds' \\ & -\frac{\sin\tilde{k}(l+s)}{\sin 2\tilde{k}l + \alpha P^a(kr,2\tilde{k}l)}\int_{-l}^{l} E_{0s}^a(s')\sin\tilde{k}(l-s')\,ds'\Bigg\}, \end{aligned} \tag{7}$$

where P^s and P^a are the functions of vibrator eigenfield equal to

$$P^{\left\{\begin{smallmatrix} s \\ a \end{smallmatrix}\right\}}(kr,2\tilde{k}l) = \int_{-l}^{l}\left[\frac{e^{-ikR(s',-l)}}{R(s',-l)} \pm \frac{e^{-ikR(s',l)}}{R(s',l)}\right]\sin\tilde{k}(s-s')\,ds', \tag{8}$$

$\tilde{k} = k + i(\alpha/r)\bar{Z}_S$, $\bar{Z}_S = \bar{R}_S + i\bar{X}_S = 2\pi r z_i/Z_0$ is the distribution surface impedance of the vibrator, normalized to $Z_0 = 120\pi$ Ohm.

Let us consider now the problem of the vibrator excitation by a concentrated electromotive force with amplitude V_0 in its geometrical center. The model of excitation can be represented as

$$E_{0s}(s) = E_{0s}^s(s) = V_0\delta(s-0), \tag{9}$$

where $\delta(s-0) = \delta(s)$ is Dirac delta-function. Then expression (7) for the current can be written as

$$J(s) = J^s(s) = J_0^{Fs} f(s) = -\alpha V_0 \left(\frac{i\omega}{2\tilde{k}}\right) \frac{\sin\tilde{k}(l-|s|)}{\cos\tilde{k}l + \alpha P^{Fs}(kr,\tilde{k}l)}. \tag{10}$$

Using the generalized integral functions [17] and expression (2) the function $P^{Fs}(kr,\tilde{k}l) = \int\limits_{-l}^{l} \frac{e^{-ikR(s,l)}}{R(s,l)} \cos\tilde{k}s ds$ can be written in explicit form:

$$P^{Fs}(kr,\tilde{k}l)\Big|_{\frac{r}{\lambda}\ll 1} \approx \frac{1}{2}\left\{\begin{array}{l} \cos\tilde{k}l\left[\begin{array}{l} 2\ln(4l/r) - \mathrm{Cin}(2\tilde{k}l+2kl) - \mathrm{Cin}(2\tilde{k}l-2kl) \\ -i[\mathrm{Si}(2\tilde{k}l+2kl) - \mathrm{Si}(2\tilde{k}l-2kl)] \end{array}\right] \\ +\sin\tilde{k}l\left[\begin{array}{l} \mathrm{Si}(2\tilde{k}l+2kl) + \mathrm{Si}(2\tilde{k}l-2kl) \\ -i[\mathrm{Cin}(2\tilde{k}l+2kl) - \mathrm{Cin}(2\tilde{k}l-2kl)] \end{array}\right] \end{array}\right\}, \tag{11}$$

where $\mathrm{Si}(x)$ and $\mathrm{Cin}(x)$ are the integral sine and cosine of a complex argument.

The current distribution (10) allows calculation of electrodynamic characteristics of the impedance vibrator in free space. For example, the input impedance of the vibrator at the feed point is

$$Z_{in}[\mathrm{Ohm}] = \frac{V_0}{J(0)} = \left(\frac{60i\tilde{k}}{\alpha k}\right) \frac{\cos\tilde{k}l + \alpha P^{Fs}(kr,\tilde{k}l)}{\sin\tilde{k}l}. \tag{12}$$

If the vibrator is located horizontally at a distance h above the infinite perfectly conducting plane, the function $G_{0s}^{Hs}(s,s')$ in formula (6) has the following form

$$G_{0s}^{Hs}(s,s') = -\frac{e^{-ik\sqrt{(s-s')^2+(2h+r)^2}}}{\sqrt{(s-s')^2+(2h+r)^2}} = -\frac{e^{-ikR_h(s,s')}}{R_h(s,s')}. \tag{13}$$

Then, the expressions for the current and input impedance of the vibrator are

$$J(s) = J_0^{Hs} f(s) = -\alpha V_0 \left(\frac{i\omega}{2\tilde{k}}\right) \frac{\sin\tilde{k}(l-|s|)}{\cos\tilde{k}l + \alpha P^{Hs}[k(r+h),\tilde{k}l]}, \tag{14}$$

$$Z_{in}[\mathrm{Ohm}] = \frac{V_0}{J(0)} = \left(\frac{60i\tilde{k}}{\alpha k}\right) \frac{\cos\tilde{k}l + \alpha P^{Hs}(kr,\tilde{k}l)}{\sin\tilde{k}l}. \tag{15}$$

In formulas (14)–(15) the function $P^{Hs}(k(h+r),\tilde{k}l) = \int\limits_{-l}^{l} \frac{e^{-ikR_h(s,l)}}{R_h(s,l)} \cos\tilde{k}s ds$ can also be represented in explicit form

$$P^{Hs}(k(h+r),\tilde{k}l)\Big|_{\frac{r}{2l}\ll 1} \approx P^{Fs}(kr,\tilde{k}l) - \frac{1}{2}\left\{\begin{array}{l} \cos\tilde{k}l\left[\begin{array}{l} \ln\dfrac{B+2kl}{B-2kl} + \mathrm{Cin}(B-2kl) - \mathrm{Cin}(B+2kl) \\ -i[\mathrm{Si}(B+2kl) - \mathrm{Si}(B-2kl)] \end{array}\right] \\ +\sin\tilde{k}L\left[\begin{array}{l} \mathrm{Si}(B+2kl) + \mathrm{Si}(B-2kl) - 2\mathrm{Si}(A) \\ -i[\mathrm{Cin}(B+2kl) + \mathrm{Cin}(B-2kl) - 2\mathrm{Cin}(A)] \end{array}\right] \end{array}\right\}, \tag{16}$$

where $A = k(2h+r)$ and $B = \sqrt{(2kl)^2 + A^2}$.

Figure 2 shows the results of comparative calculations of the vibrator eigenfield functions $P^{Fs}(kr,\tilde{k}l)$ and $P^{Hs}(k(h+r),\tilde{k}l)$ by the numerical integration and by the approximate relations (11) and (16). As

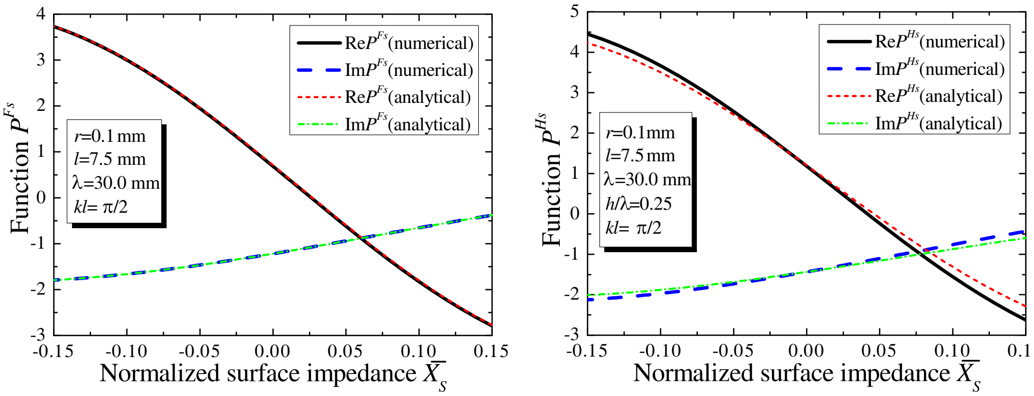

Figure 2. The functions of the vibrator eigenfield, versus the surface impedance value.

can be seen, the coincidences of the numerical and analytical values are satisfactory, especially at the relatively low values of the surface impedance.

As shown in [13], the resonant electrical length of a half-wave vibrator with account of diffraction effects at the screen edges coincides with the resonant length of an electric vibrator above the infinite plane if the screen size greater than the wavelength. In our problem, we may assume that for the screen dimensions comparable to or greater than the wavelength, the influence of the diffracted field upon the vibrator current can be small. Therefore, the current in Eq. (6) can be found setting $G^D_{0s}(s,s') = 0$. The influence of the screen edges on the total field amplitude will be taken into account by the diffracted fields using UGTD according to Eq. (1). Further, we will use this approach.

3.2. Resonant Properties of Impedance Vibrators

Since resonances are observed, when the imaginary part of the vibrator input impedance in Eq. (12) is equal to zero ($X_{in} = 0$), we arrive at the transcendental equation for the resonant electrical length of the impedance vibrator in the free space

$$\cos(\tilde{k}l)_{res} + \alpha \mathrm{Re}P^{Fs}\left[kr, (\tilde{k}l)_{res}\right] = 0, \tag{17}$$

where $\mathrm{Re}P^{Fs}$ is the real part of the function P^{Fs}, defined by Eq. (11).

Let us find an approximate solution of Equation (17), expanding the unknown quantity in powers of the small parameter α

$$(\tilde{k}l)_{res} = (\tilde{k}l)_0 + \alpha(\tilde{k}l)_1 + \alpha^2(\tilde{k}l)_2 + \dots \tag{18}$$

Substituting Eq. (18) into Eq. (17) and equating terms of equal powers of α, up to terms of order α^2, we have:

$$(\tilde{k}l)_{res} \approx \frac{\pi}{2} + \alpha \mathrm{Re}P^{Fs}\left(\frac{\pi r}{2l}, \frac{\pi}{2}\right) = \frac{\pi}{2} + \frac{\alpha}{2}\left[\mathrm{Si}\left(2\pi + \alpha\frac{2l}{r}\bar{X}_{Sres}\right) - \mathrm{Si}\left(\alpha\frac{2l}{r}\bar{X}_{Sres}\right)\right]. \tag{19}$$

The formula for the value of the surface impedance of the resonant vibrator in the free space, depending on its dimensions and the wavelength, can be obtained by setting $\bar{X}_{Sres} \sim \frac{r}{2l}$ as:

$$\bar{X}^{Fs}_{Sres} = \frac{\Omega r}{l}\left[\frac{\pi}{2} - kl - \frac{\mathrm{Si}(2\pi)}{2\Omega}\right], \quad \Omega = 2\ln\frac{2l}{r}. \tag{20}$$

Analogously, $\bar{X}^{Hs}_{Sres}$ for the vibrator over the plane may be presented as

$$\bar{X}^{Hs}_{Sres} = \frac{\Omega r}{l}\left[\frac{\pi}{2} - kl - \frac{\mathrm{Si}(2\pi) - \mathrm{Si}\left(\pi\sqrt{1+(h/l)^2}+\pi\right) - \mathrm{Si}\left(\pi\sqrt{1+(h/l)^2}-\pi\right) + 2\mathrm{Si}\left(\pi(h/l)\right)}{2\Omega}\right]. \tag{21}$$

Formulas defining specific realizations of the vibrator surface impedance are given in Appendix A.

4. DETERMINATION OF GO AND DIFFRACTED FIELDS

4.1. Field Radiation Pattern for the Impedance Vibrator in Free Space and over the Plane

The field RP of an arbitrarily oriented impedance vibrator in the free space ($\varepsilon_1 = \mu_1 = 1$) can be found by substituting expression for the current Eq. (10) into the formula for the Hertz vector potential in the far zone and integrating it over the length of the vibrator. If the observation angle θ is measured from the axis Z, the RP of impedance vibrator **1**, parallel to the axis Z, has the following form

$$F_{\|}(\theta) = k\tilde{k}\sin\theta\frac{\cos\tilde{k}l - \cos(kl\cos\theta)}{(k\cos\theta)^2 - \tilde{k}^2}. \tag{22}$$

The RP of the vibrator oriented at an angle ζ to the axis X, i.e., for vibrators **2** and **3** (Fig. 1), can be presented as

$$F_{\perp}(\theta,\varphi) = k\tilde{k}\frac{\cos\tilde{k}l - \cos(kl\cos\theta')}{(k\cos\theta')^2 - \tilde{k}^2}, \tag{23}$$

where $\cos\theta' = \sin\theta\cos(\varphi-\zeta)$. For the vibrator **2** and **3** the angle ζ is equal to $\pi/2$ and zero, respectively. Taking into account of Eq. (22), the far field of the impedance vibrator **1** in the spherical coordinate system ρ, θ, φ associated with the middle of the vibrator has only one component

$$E_{\theta\infty}(\theta) = i\frac{J_0^{Fs}Z_0}{2\pi}\frac{\exp(-ik\rho)}{\rho}F_{\|}(\theta), \tag{24}$$

where J_0^{Fs} is the current amplitude of the impedance vibrator in the free space (10).

If the impedance vibrator **1** is located at a distance h from a perfectly conducting plane, the far field of the incident and reflected waves ($p = 1, 2$) in the coordinate system $\tilde{R}, \theta, \varphi$ associated with the plane according to the boundary condition and the expression (24) has the following form

$$E_{\theta p\|}(\theta,\varphi) = (-1)^{p+1}\, i\frac{J_0^{Hs}Z_0}{2\pi}\frac{\exp(-ik\rho_p)}{\rho_p}F_{\|}(\theta). \tag{25}$$

Here J_0^{Hs} is the amplitude of current on the impedance vibrator in the presence of a perfectly conducting plane (14), and ρ_p is the distance from the GO wave radiator ($p = 1, 2$) to the observation point.

The eikonals of the incident s_{inc} and reflected s_{ref} waves are equal

$$s_{inc,ref} = \rho_p = \left[h^2 + \tilde{R}^2 - 2\tilde{R}h\sin\theta\cos\left(\varphi - \varphi_{0p}\right)\right]^{1/2}, \tag{26a}$$

where $\varphi_{0p} = 0$ and π are elevation angles of the radiators $p = 1, 2$ in the coordinate system $\tilde{R}, \theta, \varphi$. In the far field in the dominator of Eq. (25) $\rho_p = \tilde{R}$ and the eikonals of the incident s_{inc} and s_{ref} reflected waves in the phase factor of Eq. (26a) take the form

$$s_{inc,ref} = \tilde{R} - h\sin\theta\cos\left(\varphi - \varphi_{0p}\right). \tag{26b}$$

The final expressions for the incident and reflected fields in the GO approximation when the screen is excited by the vibrator **1** can be written, using the expressions (25)–(26b) in the form

$$E_{\theta\|p}(\theta,\varphi) = (-1)^{p+1}J_0^{Hs}E_0F_{\|}(\theta)\exp(ik\delta_p), \tag{27a}$$

where

$$E_0 = 60i\frac{\exp(-ik\tilde{R})}{\tilde{R}}, \quad \delta_p = h\sin\theta\cos\left(\varphi - \varphi_{0p}\right), \tag{27b}$$

δ_p is the path difference of parallel rays passing from the origin O in the coordinate system $\tilde{R}, \theta, \varphi$ and from the middle of the p-th GO wave radiator in the observation direction (θ, φ); $F_{\|}(\theta)$ is the RP of the impedance vibrator **1** in the free space (22).

The electric field vector for the vibrator **2** in the same coordinate system has two components [6]

$$E_{\theta\perp p}(\theta,\varphi) = -J_0^{Hs}E_0F_{\perp}(\theta,\varphi)\cos\left(\varphi - \zeta_p\right)\cos\theta\exp\left(ik\delta_p\right), \tag{28a}$$

$$E_{\varphi\perp p}(\theta,\varphi) = J_0^{Hs}E_0F_{\perp}(\theta,\varphi)\sin\left(\varphi - \zeta_p\right)\exp\left(ik\delta_p\right), \tag{28b}$$

where $F_{\perp}(\theta,\varphi)$ is the RP for the impedance vibrator **2** in the free space (23); the angles $\zeta_p = \pi/2$ $(p = 1)$, $\zeta_p = 3\pi/2$ $(p = 2)$.

4.2. Fields of Waves Diffracted on the Screen Edges

Let us now define the fields of impedance vibrator **1** diffracted by four sharp edges of the perfectly conducting rectangular screen. Let us introduce the rectangular proper coordinate systems (PCS) $X_nY_nZ_n$ at each edge of the screen (see Fig. 1) so that the X_n axis lies in the plane of the screen; the axis Z_n is directed along its edge; the middle of the vibrator is in a plane X_nY_n. In the spherical coordinate systems R_n, θ_n, φ_n, associated with the rectangular PCS, the angles θ_n and φ_n are measured from the axes Z_n and X_n, respectively. A virtual diffraction radiator is allocated on each edge of the screen in the PCS origin. The RP of the radiator corresponds to that of the edge wave which is excited by the Hertz dipole field at the edge of the perfectly conducting half-plane. Expressions for the components of the edge wave field in the far zone, uniform for all observation angles, are obtained using the approximation of rigorous solutions [18] by zero terms of their asymptotic expansions on degrees of $(k\rho)^{-1}$ in the PCS on the edge of the half-plane. Approximation expressions of field components for the dipoles parallel and perpendicular to the half-plane edge are valid for any distance r_0 between the dipole and the half-plane edge if the inequality $\tilde{R} \gg r_0$ holds.

If the n-th screen edge is excited by the vibrator parallel to this edge, the asymptotic fields of unit edge waves excited by the incident and reflected waves ($p = 1, 2$) in the coordinate system R_n, θ_n, φ_n are the product of the GO field amplitude $E_{\theta\|p}(\theta_n, \varphi_n)$ in the observation direction and function $T(\xi_{pn})$ describing transition from light to shadow regions of the GO waves [6]

$$E_{\theta\|pn}\left(\theta_n, \varphi_n\right) = E_{\theta\|p}\left(\theta_n, \varphi_n\right) T\left(\xi_{pn}\right). \tag{29}$$

If the n-th screen edge is excited by the vibrator perpendicular to this edge, the uniform approximation of diffracted field excited by the incident wave ($p = 1$) has the form

$$\begin{aligned} E_{\theta\perp pn}\left(\theta_n, \varphi_n\right) &= E_{\theta\perp p}\left(\theta_n, \varphi_n\right) T\left(\xi_{pn}\right) - \sqrt{\frac{2}{\pi k r_{pn}\sin\theta_n}}\cos\theta_n \sin\frac{\varphi_n}{2}\sin\left(\gamma_{pn} - \frac{\varphi_{pn}}{2}\right) \\ &\quad \times \exp\left[-i\left(k r_{pn}\sin\theta_n + \pi/4 - k\delta_n\right)\right], \end{aligned} \tag{30a}$$

$$\begin{aligned} E_{\varphi\perp pn}\left(\theta_n, \varphi_n\right) &= E_{\varphi\perp p}\left(\theta_n, \varphi_n\right) T\left(\xi_{pn}\right) - \sqrt{\frac{2}{\pi k r_{pn}\sin\theta_n}}\cos\frac{\varphi_n}{2}\sin\left(\gamma_{pn} - \frac{\varphi_{pn}}{2}\right) \\ &\quad \times \exp\left[-i\left(k r_{pn}\sin\theta_n + \pi/4 - k\delta_n\right)\right], \end{aligned} \tag{30b}$$

while the diffracted field excited by the reflected wave ($p = 2$), can be written as

$$E_{\theta\perp pn}\left(\theta_n, \varphi_n\right) = E_{\theta\perp p}\left(\theta_n, \varphi_n\right) T\left(\xi_{pn}\right), \quad E_{\varphi\perp pn}\left(\theta_n, \varphi_n\right) = E_{\varphi\perp p}\left(\theta_n, \varphi_n\right) T\left(\xi_{pn}\right). \tag{30c}$$

Here $E_{\theta\|p}(\theta_n, \varphi_n)$, $E_{\theta\perp p}(\theta_n, \varphi_n)$, $E_{\varphi\perp p}(\theta_n, \varphi_n)$ are the GO field components in the material medium surrounding the vibrator; r_{pn}, φ_{pn} are the polar coordinates of the p-th GO wave radiator in the PCS on the n-th edge; γ_{pn} is the angle between the axis of the p-th radiator and O_nX_n axis. The polar coordinates of the p-th radiator in the PCS are

$$r_{pn} = \left(x_{pn}^2 + y_{pn}^2 + z_{pn}^2\right)^{1/2}, \quad \varphi_{pn} = \mathrm{arctg}(y_{pn}/x_{pn}). \tag{31a}$$

For the problem geometry of Fig. 1, the radius vector for the p-th GO radiator in the PCS on the lateral 1, 2 and transverse edges 3, 4 can be written as

$$r_{1,2} = \sqrt{h^2 + (L/2)^2}, \quad r_{3,4} = \sqrt{h^2 + (W/2)^2}\,. \tag{31b}$$

4.3. Transition Functions from Light to Shadow

The uniform field asymptotics for the edge waves in Eqs. (29)–(30c) contain the transition function from light to shadow $T(\xi_{pn})$ for the incident ($p = 1$) and reflected ($p = 2$) waves diffracted at the n-th screen edge

$$T\left(\xi_{pn}\right) = \pm\frac{\Phi\left(\left|\xi_{pn}\right|\sqrt{i}\right) - 1}{2}, \quad \Phi\left(\xi_{pn}\sqrt{i}\right) = 2\pi^{-1/2}\exp\left(i\pi/4\right)\int\limits_0^{\xi_{pn}}\exp\left(-it^2\right)dt, \tag{32a}$$

where "+" and "−" signs are used respectively in the light and shadow regions of the GO fields. Here $\Phi(|\xi_{pn}|\sqrt{i})$ is the probability integrals of complex arguments, where

$$|\xi_{1n}| = \sqrt{k(s_{ed_{1n}} - s_{inc})}, \quad |\xi_{2n}| = \sqrt{k(s_{ed_{2n}} - s_{ref})}. \tag{32b}$$

Here, $s_{ed_{2pn}}$ is eikonal of the edge wave, excited by the p-th GO radiator on the n-th edge, and s_{inc} and s_{ref} are eikonals of the incident or reflected waves, determined by formulas (26a)–(26b).

The edge wave eikonal $s_{ed_{pn}}$ is equal to the sum of optical paths s'_{pn} along the GO ray from the p-th source to the diffraction point Q on the n-th screen edge, and s_{pn} from the point Q to the observation point $M(\theta_n, \varphi_n)$ along the diffracted ray QM

$$s_{ed_{pn}} = s'_{pn} + s_{pn}, \quad s'_{pn} = r_{pn}/\sin\theta_n. \tag{33}$$

In the far-field arguments in Eq. (32b), expressions for ξ_{pn} can be simplified

$$|\xi_{pn}| = \sqrt{2kr_{pn}\sin\theta_n}\cos\frac{\varphi_n - \varphi_{pn}}{2}. \tag{34}$$

Here we have taken into account the ratio in Eq. (33) and the facts that the distance $s_{pn} = \tilde{R} - \frac{r_{pn}\cos^2\theta_n}{\sin\theta_n}$, while $s_{inc,ref}$ are defined by formula (26b), and r_{pn} and φ_{pn} by formulas (31a)–(31b).

When GO wave crosses the light-shadow boundaries $\varphi_n = \pi - \varphi_{pn}$ in the PCS, argument of the probability integral ξ_{pn} in Eq. (34) changes its sign. Since the probability integral is antisymmetrical, the sign of the transition function $T(\xi_{pn})$ in Eq. (32a) also changes its sign. At the light-shadow boundaries, the argument of the probability integral is $\xi_{pn} = 0$, hence $\Phi(0) = 0$ and $T(0) = \pm 1/2$. Owing to this jump in the phase of unite edge wave, the amplitude of the total field at the light-shadow boundary of the GO waves remains continuous. Following from Eqs. (32a) and (34), the functions $T(\xi_{pn})$ for the incident and reflected waves depend on the wavelength, medium parameters, vibrator position (r_{pn}, φ_{pn}) relative to the screen edge, and observation direction (θ_n, φ_n).

4.4. GO Fields in the Coordinate Systems on the Screen Edges

The diffracted fields are defined in the PCS on n-th edge by expressions (29)–(30c), depending on the fields of the incident and reflected waves in the observation direction (θ_n, φ_n). The expressions for the GO fields of the vibrator parallel to the screen edge can be defined using Eq. (27a) as

$$E_{\theta\| pn}(\theta_n, \varphi_n) = (-1)^{p+1} J_0^{Hs} E_0 F_\|(\theta_n) \exp\left[ik(\delta_n + \delta_{pn})\right], \tag{35}$$

and for the vibrator perpendicular to the screen edge can be written using Eqs. (28a)–(28b)

$$E_{\theta\perp p}(\theta_n, \varphi_n) = -J_0^{Hs} E_0 F_\perp(\theta_n, \varphi_n)\cos(\varphi_n - \gamma_{pn})\cos\theta_n \exp\left[ik(\delta_n + \delta_{pn})\right], \tag{36a}$$

$$E_{\varphi\perp pn}(\theta_n, \varphi_n) = J_0^{Hs} E_0 F_\perp(\theta_n, \varphi_n)\sin(\varphi_n - \gamma_{pn}) \exp\left[ik(\delta_n + \delta_{pn})\right]. \tag{36b}$$

The terms in the exponentials of expressions (35)–(36b) are defined as follows: δ_{pn} is the path difference for the rays passing from the middle of the p-th radiator and from the PCS origin O_n on the n-th screen edge in the observation direction (θ_n, φ_n); δ_n is the path difference for the rays passing from the origin O and from the point O_n in the coordinate system R, θ, φ in the observation direction

$$\delta_{pn} = r_{pn}\sin\theta_n\cos(\varphi_n - \varphi_{pn}), \quad \delta_n = x_{0n}\sin\theta\cos\varphi + y_{0n}\sin\theta\sin\varphi + z_{0n}\cos\theta. \tag{37}$$

The rectangular coordinates x_{0n}, y_{0n}, z_{0n} of the PCS origin O_n on n-th screen edge in the coordinate system XYZ with origin at the screen middle are equal to

$$x_{01,2} = 0,\ y_{01,2} = \pm L/2,\ z_{01,2} = 0 (n = 1, 2); x_{03,4} = 0,\ y_{03,4} = 0,\ z_{03,4} = \pm W/2 (n = 3, 4). \tag{38}$$

The RP of the impedance vibrator $F_\|(\theta_n)$ and $F_\perp(\theta_n, \varphi_n)$ in Eqs. (35) and (36a)–(36b) can be obtained using Eqs. (22) and (23), and replacing the angles θ and θ' by θ_n and θ'_n, φ, ζ by φ_n and γ_{pn}.

The components of diffracted field defined in the PCS on the n-th screen edge are projected on the axis of the coordinate system R, θ, φ and are summarized according to Eq. (1).

5. NUMERICAL RESULTS

As shown above, the electric vibrator of fixed geometrical sizes $(2l, r)$ located above the screen at the distance h can be tuned to resonance using the surface impedance $\bar{X}_{Sres}$. For practical applications, it is important to know the values of $\bar{X}_{Sres}$ depending on the distance between the screen and vibrator having different electrical lengths, and corresponding radiation characteristics. There are some criteria for determining the values of the resonant surface impedance $\bar{X}_{Sres}$: the maximum field amplitude and equality to zero the reactive part of the input impedance X_{in}. In this paper, the resonant impedance as a function of the relative distance between the vibrator and screen is determined by formula (21) derived from the condition $X_{in} = 0$ for the vibrator placed over the infinite-plane (in this approximation $\bar{X}_{Sres} = \bar{X}^{Hs}_{Sres}$).

The resonance values $\bar{X}_{Sres}$ and corresponding to them the field intensity $|E_n|^2$ and directive gain D along the normal to the screen, depending on the distance between the screen and vibrator h/λ, were calculated for the electrical impedance vibrators with lengths $2l/\lambda$=0.4, 0.5 and 0.6. The directive gain was found using the formula

$$D(0,0) = 120\frac{|E_n|^2}{R_\Sigma}, \tag{39}$$

where $R_\Sigma = 30 I_\Sigma/\pi$, $I_\Sigma = \int\limits_0^{2\pi} d\varphi \int\limits_0^{\pi} f^2(\theta,\varphi)\sin\theta d\theta$, $f^2(\theta,\varphi) = |f_\theta(\theta,\varphi)|^2 + |f_\varphi(\theta,\varphi)|^2$, $f_\theta(\theta,\varphi)$ and $f_\varphi(\theta,\varphi)$ are the RP-s for the orthogonal linear polarized field components. All numerical results are given for the horizontal vibrator **1** with radius $r = 0.1$ mm at the wavelength of 30 mm.

To determine the influence of the surface impedance upon the far zone field of the vibrators with various lengths, the normalized field intensity $|E_n|^2/|E_{n\max}|^2$ in the normal direction to the perfectly conducting plane was calculated in dependence on the surface impedance $\bar{X}_S$, which varies within ± 0.15 (Fig. 3). The electrical length of the vibrator $2l/\lambda$ was equal to 0.4, 0.5 and 0.6, and the distance between the vibrator and the plane was equal $h = 0.25\lambda$.

Figure 3 shows that the maximum amplitude of the field, i.e., resonance, occurs at different values of the surface impedance, depending on the vibrator length. The maximum amplitudes correspond to the resonant impedance $\bar{X}^{Hs}_{Sres}$ equaled to 0.033, -0.012, and -0.043 when the $2l$ is equal to 0.4λ, 0.5λ, and 0.6λ, respectively. Thus, the resonance can be observed for the positive impedance (inductive type) if the vibrator electrical length is less than the half-wavelength and for the negative impedance (capacitive type) if the vibrator length is equal to or greater than half-wavelength.

Figure 4 shows the resonant values of the surface impedance $\bar{X}^{Hs}_{Sres}$ for the vibrators with the same length located over the plane versus the distance h/λ between the vibrator and screen that varies within

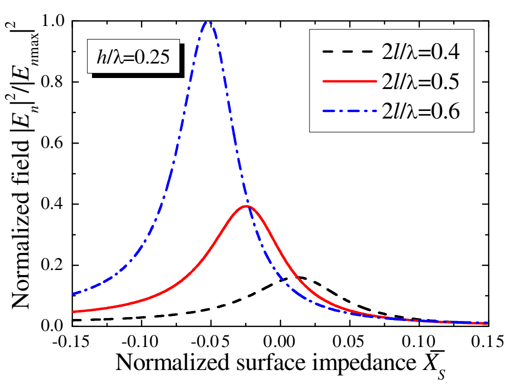

Figure 3. Normalized field intensity versus vibrator normalized surface impedance.

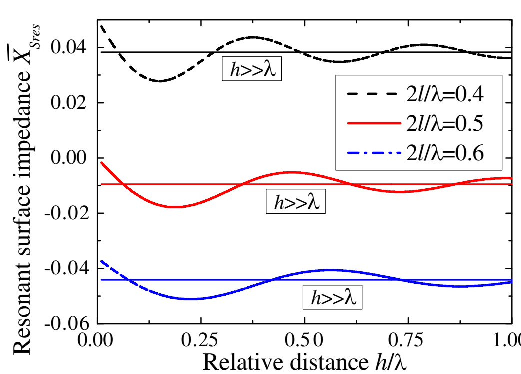

Figure 4. Resonant values of the vibrator surface impedance versus the distance between the vibrator and plane h/λ, straight lines correspond to the case vibrators location in free space and referred to as $h \gg \lambda$.

$0.1\div1$. The values were calculated using formula (21) and the condition $X_{in} = 0$. When $h = 0.25\lambda$ we have for the vibrators with length 0.4λ, 0.5λ, and 0.6λ that $\bar{X}^{Hs}_{Sres}$ is equal to 0.035, -0.016 and -0.051, respectively. Fig. 4 also shows the surface impedance values $\bar{X}^{Fs}_{Sres}$ for the resonant vibrator in the free space ($h \gg \lambda$), calculated using the formula (20). Depending on the vibrator length we have: $\bar{X}^{Fs}_{Sres}$ is equal to 0.038, -0.01, and -0.044 if the $2l$ is 0.4λ, 0.5, and 0.6λ, respectively.

Figure 5 shows the dependences of the normalized field intensity $|E_n|^2/|E_{n\,\max}|^2$ in the normal

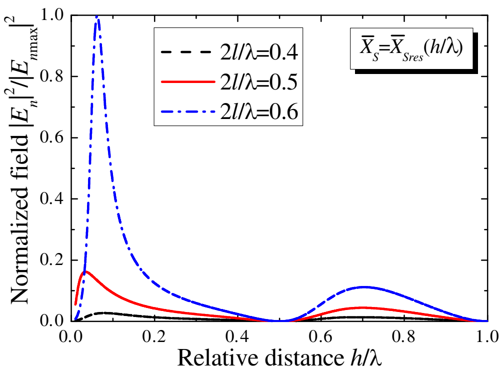

Figure 5. Normalized field intensity versus the distance between the vibrator and plane h/λ.

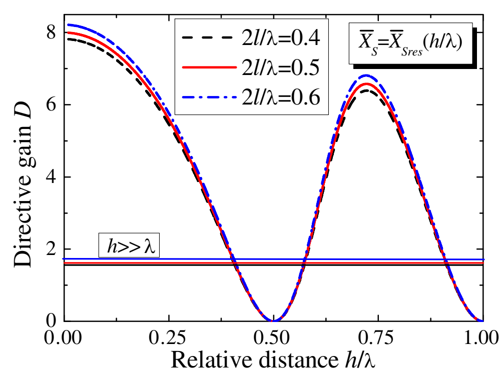

Figure 6. Directive gain versus the distance between the vibrator and plane, straight lines correspond to the case vibrators location in free space and referred to as $h \gg \lambda$.

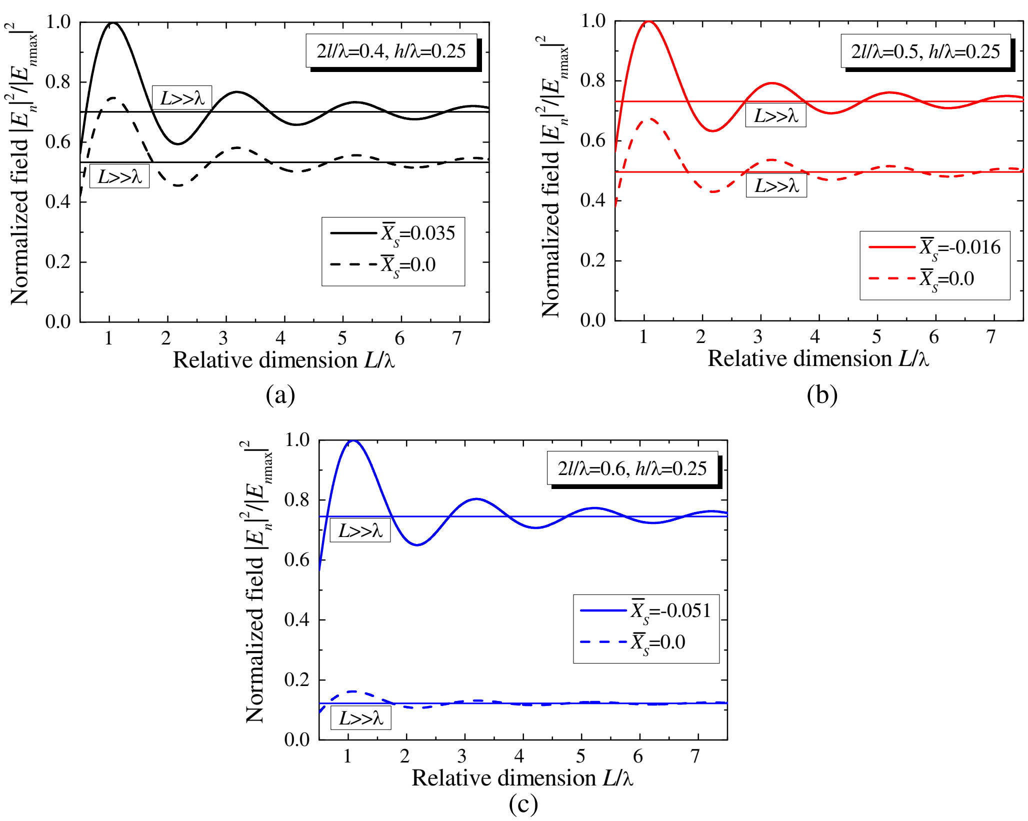

Figure 7. The normalized field intensity versus the screen dimensions, straight lines correspond to the case vibrators location over an infinite plane and referred to as $L \gg \lambda$.

direction to the plane on the distance h/λ for the resonant vibrators with 0.4λ, 0.5, and 0.6λ of length $2l$. The maximum field intensity $|E_{n\,\max}|^2$ is achieved at $2l = 0.6\lambda$. The impedance $\bar{X}^{Hs}_{Sres}$ for each h/λ corresponds to that in Fig. 4. The maximum of field intensity reaches at following $h_{\max}/\lambda$: 0.124, 0.101, and 0.087 if the $2l$ is equal to 0.4λ, 0.5λ, and 0.6λ, while the impedance of the resonant vibrators $\bar{X}^{Hs}_{Sres}$ being 0.028, -0.0148 and -0.045, respectively (Fig. 4). For the above $h_{\max}/\lambda$ values, the R_Σ for the vibrator **1** are small, which leads to large values of the directive gain D (see Fig. 6).

Figure 6 illustrates varying the directive gain D of the resonant impedance vibrators with length $2l$ equal to 0.4λ, 0.5, and 0.6λ in the normal direction to the perfectly conducting plane depending on the distance h/λ. This figure also shows the D-values in the free space ($h \gg \lambda$) that are equal to 1.59, 1.64 and 1.74 if the $2l$ is equal to 0.4, 0.5 and 0.6, respectively. Character of varying D-values as functions of h/λ is defined by the RP of the vibrator **1**. The maximum occurs at distances h equal to an odd number of quarter waves, while the zero minima are at an integer number of half wavelengths. At the distance $h = 0.25\lambda$, the D-values of the resonant impedance vibrators, with length $2l/\lambda$ equal to 0.4, 0.5 and 0.6, reaches 5.45, 5.6 and 5.76, respectively. These values coincide with that of the perfectly conducting vibrator located above the plane [6].

Let us compare the normalized field intensity $|E_n|^2/|E_{n\,\max}|^2$ of the resonant impedance vibrator ($\bar{X}_S = \bar{X}^{Hs}_{Sres}$, see Fig. 4) and perfectly conducting vibrator ($\bar{X}_S = 0$) of the same electrical length located at $h = 0.25\lambda$ above a perfectly conducting screen with sizes $L = W$ (see Fig. 1). Figs. 7(a)–7(c) show the values of $|E_n|^2/|E_{n\,\max}|^2$ for the vibrators with lengths $2l/\lambda$ equal to 0.4, 0.5 and 0.6 depending on the relative screen dimension L/λ. These figures also show the $|E_n|^2/|E_{n\,\max}|^2$ in the case of the vibrators located over the plane ($L \gg \lambda$).

The calculations have shown that the maximum of field intensity for the impedance and perfectly conducting vibrators if the current $J_0^{Hs} f(s)$ is defined by Eq. (14) does not depend upon the vibrator length. The maximum of field is achieved at the optimal screen dimensions L_{opt} being in the range $1.05 \div 1.1\lambda$. Significant differences between $|E_n|^2/|E_{n\,\max}|^2$ for the impedance and perfectly conducting vibrators are observed when their length $2l = 0.6\lambda$.

Figure 8 shows the dependences of the normalized field intensity $|E_n|^2/|E_{n\,\max}|^2$ for the resonant vibrators of the same lengths on the screen dimensions L/λ, when the distances between the vibrator and screen $h_{\max}/\lambda$ (see Fig. 5) ensure the maximum field amplitude. In this case, the optimal screen dimension L_{opt} is equal to 1.2λ for the half-wave vibrator and 1.15λ for vibrator with 0.4λ and 0.6λ of length $2l$.

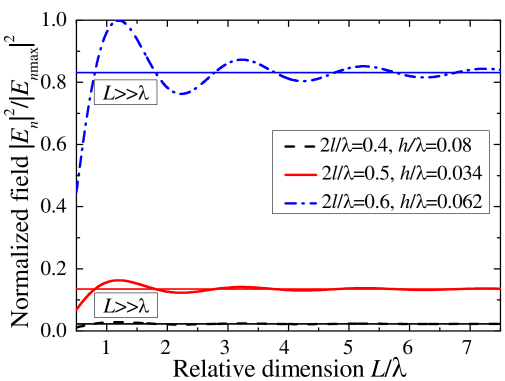

Figure 8. The normalized field intensity versus the screen dimensions, straight lines correspond to the case vibrators location over an infinite plane and referred to as $L \gg \lambda$.

6. CONCLUSION

The paper presents the solution to the problem of electromagnetic waves radiation by the vibrator with distributed along its length surface impedance. The vibrator is located above the perfectly conducting rectangular screen of finite size. The solution is derived based on the asymptotic expression for the current in the horizontal impedance vibrator over the perfectly conducting infinite plane, obtained by averaging method. The problem is solved under the assumption that the influence of the fields diffracted by the screen edges upon the current amplitude in the vibrator is negligible. This assumption is valid when the screen dimensions are comparable with or greater than the wavelength. The full radiation field of the analyzed structure for all viewing angles in the far zone was found by uniform geometrical theory of diffraction. Multiparameter study of the electrodynamic characteristics for the resonant impedance vibrators located over the infinite plane and square screen, depending on the size of the vibrator, the value and type of the surface impedance, removing from the screen and the screen dimensions are presented. The research results can be useful in the design of radiating systems, part of which are thin vibrators and finite dimensional screens.

APPENDIX A. SURFACE IMPEDANCE OF VIBRATORS

Formulas determining the distributed surface impedance of electrically thin vibrators (material parameters are ε, μ, σ) have the following form

No	The vibrator design	Vibrator model	Impedance
1	Solid metal cylinder. The radius satisfy inequality $r \gg \Delta^0$, Δ^0 is skin layer thickness.		$\bar{Z}_S = \dfrac{1+i}{120\pi\sigma\Delta^0}$
2	Metallized dielectric cylinder. Metal layer thickness is $h_R \ll \Delta^0$.		$\bar{Z}_S = \dfrac{1}{120\pi\sigma h_R + ikr(\varepsilon-1)/2}$
3	Metal-dielectric cylinder. L_1 is the thickness of a metal discs, L_2 is the thickness of a dielectric disks.		$\bar{Z}_S = -i\dfrac{L_2}{L_1+L_2}\dfrac{2}{kr\varepsilon}$
4	Magnetodielectric metalized cylinder. r_i is the radius of internal conducting cylinder.		$\bar{Z}_S = \dfrac{1}{120\pi\sigma h_R - i/kr\mu\ln(r/r_i)}$
5	Metal cylinder coated with magnetodielectric layer, which thickness is $r-r_i$, or corrugated cylinder $(L_1+L_2) \ll \lambda$, where L_1 is crests thickness where $\bar{Z}_S=0$, L_2 is the notch width where $\bar{Z}_S \neq 0$.	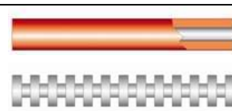	$\bar{Z}_S = ikr\mu\ln(r/r_i)$
		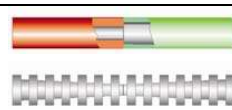	$\bar{Z}_S(s) = \bar{Z}_S\phi(s)$
6	Metal monofilar helix. r is helix radius $kr \ll 1$, ψ is winding angle.		$\bar{Z}_S = (i/2)kr\,\mathrm{ctg}^2\,\psi$

Formulas for surface impedances of vibrators obtained in the frame of the impedance concept [10] and are valid for thin cylinders $|(k\sqrt{\varepsilon\mu r})^2\ln(k\sqrt{\varepsilon\mu r_i})| \ll 1$ both for finite and infinite cylinders, located in the hollow electrodynamic volume. If vibrators are in a material medium with parameters ε_1 and μ_1, all above formulas must contain the factor $\sqrt{\mu_1/\varepsilon_1}$.

REFERENCES

1. Keller, J. B., "Diffraction by aperture," *J. Appl. Phys.*, Vol. 28, 570–579. 1957.

2. Keller, J. B., "Geometrical theory of diffraction," *J. Opt. Soc. of Amer.*, Vol. 52, 116–130, 1962.
3. Tsai, L. L., D. R. Wilton, M. G. Harrison, and E. H. Wright, "A comparison of geometrical theory of diffraction and integral equation formulation for analysis of reflector antennas," *IEEE Trans. Antennas and Propagat.*, Vol. 20, 705–712, 1972.
4. Kouyoumjian, R. G. and P. H. Pathak, "A uniform geometrical theory of diffraction for an edge in a perfectly conducting surface," *Proceedings of the IEEE*, Vol. 62, 1448–1461, 1974.
5. Pathak, P. H., "High frequency techniques for antenna analysis," *Proceedings of the IEEE*, Vol. 80, No. 1, 44–65, 1992.
6. Yeliseyeva, N. P. and N. N. Gorobets, *Diffraction of Radiation of the Wire Antenna on the Rectangular and Corner Screens*, V. N. Karazin Kharkiv National University, Kharkiv, 2009 (in Russian).
7. Gorobets, N. N. and N. P. Yeliseyeva, "Polarization effects caused by diffraction of the radiated of an arbitrarily oriented electric dipole at the edge of a perfectly conducting half plane," *Journal of Communication Technology and Electronics*, Vol. 51, 147–157, 2006.
8. Gorobets, N. N., N. P. Yeliseyeva, and Ye. A. Antonenko, "Optimization of radiation characteristics of wire-screened antennas," *Telecommunications and Radio Engineering*, Vol. 71, 59–69, 2012.
9. Nesterenko, M. V., "Analytical methods in the theory of thin impedance vibrators," *Progress In Electromagnetics Research B*, Vol. 21, 299–328, 2010.
10. Nesterenko, M. V., V. A. Katrich, Y. M. Penkin, V. M. Dakhov, and S. L. Berdnik, *Thin Impedance Vibrators. Theory and Applications*, Springer Science+Business Media, New York, 2011.
11. Yeliseyeva, N. P., "The input impedance of an arbitrarily oriented electric dipole located over a rectangular screen. Part 1 — The method of calculation," *Radioelectronics and Communications Systems*, Vol. 48, No. 11, 4–13, 2005.
12. Yeliseyeva, N. P., "The input impedance of an arbitrarily oriented electric dipole located over a rectangular screen. Part 2 — The calculation results," *Radioelectronics and Communications Systems*, Vol. 48, No. 12, 1–4, 2005.
13. Gorobets, N. N. and N. P. Yeliseyeva, "Metallic shield influence on the resonant length of a wire antenna," *Telecommunications and Radio Engineering*, Vol. 69, 1137–1152, 2010.
14. Khizhnyak, N. A., *Integral Equations of Macroscopical Electrodynamics*, Naukova Dumka, Kiev, 1986 (in Russian).
15. Morse, P. M. and H. Feshbach, *Methods of Theoretical Physics*, McGraw-Hill, New York, 1953.
16. Nesterenko, M. V., D. Yu. Penkin, V. A. Katrich, and V. M. Dakhov, "Equation solution for the current in radial impedance monopole on the perfectly conducting sphere," *Progress In Electromagnetics Research B*, Vol. 19, 95–114, 2010.
17. King, R. W. P., *The Theory of Linear Antennas*, Harv. Univ. Press, Cambr., MA, 1956.
18. Vandakurov, Yu. V., "Diffraction of electromagnetic waves radiated by arbitrarily oriented electric or magnetic dipole over the perfectly conducting half-plane," *J. Exp. Theor. Phys.*, Vol. 26, No. 1, 13–18, 1954 (in Russian).